Developmental and Comparative Immunology 149 (2023) 105059

Contents lists available at ScienceDirect

Developmental and Comparative Immunology

journal homepage: www.elsevier.com/locate/devcompimm

Black carp RIOK3 suppresses MDA5-mediated IFN signaling in the antiviral innate immunity

Qian Li, Lixia Xie, Jiaji Pan, Yixuan He, Enhui Wang, Hui Wu, Jun Xiao *, Hao Feng **

State Key Laboratory of Developmental Biology of Freshwater Fish, College of Life Science, Hunan Normal University, Changsha, 410081, China

ARTICLE INFO

Keywords:
RIOK3
MDA5
Innate immunity
IFN
Black carp

ABSTRACT

In mammals, right open reading frame kinase 3 (RIOK3) is related with cancer development and immune regulation. To explore the role of teleost RIOK3 in the antiviral innate immunity, the homolog of RIOK3 (bcRIOK3) from black carp (*Mylopharyngodon piceus*) has been cloned and characterized in this study. Sequence analysis revealed that bcRIOK3 is conserved in vertebrates. The transcription of bcRIOK3 varied in host cells in response to the stimulation of spring viremia of carp virus (SVCV), poly (I:C), and LPS. Immunoblotting (IB) and immunofluorescence (IF) assays identified bcRIOK3 as a cytoplasmic protein with a molecular weight of ~60 kDa. It was interesting that bcRIOK3 knockdown led to the decreased basal mRNA levels of *IFNa*, *IFNb* and *Viperin*; however, triggered obviously higher mRNA levels of the above genes after viral infection and enhanced host resistance to SVCV. Like its mammalian counterpart, bcRIOK3 overexpression in EPC cells showed a significant inhibitory effect on black carp MDA5 (bcMDA5)-mediated transcription of interferon promoters and antiviral activity. Co-immunoprecipitation and immunofluorescent assays identified the association between bcRIOK3 and bcMDA5. Further analysis revealed that bcRIOK3 enhanced the K48-linked ubiquitination and proteasome-dependent degradation of bcMDA5, and it weakened the oligomerization of bcMDA5 under poly (I:C) stimulation. In summary, our data conclude that RIOK3 dampens MDA5-mediated IFN signaling by promoting its degradation in black carp, which provide new insights into the regulation of IFN signaling in teleost.

1. Introduction

In vertebrates, the immune system plays an important role in fighting against pathogenic microbes. It encompasses both innate immunity and adaptive immunity (Akira et al., 2006). The innate immune system serves as the first line of defense against pathogens and is particularly vital for lower vertebrates. It recognizes various pathogens such as bacteria and viruses through germ-line encoded pattern recognition receptors (PRRs) (Boehm et al., 2012; Brubaker et al., 2015). In mammals, PRRs comprise toll-like receptors (TLRs), retinoic acid-inducible gene I (RIG-I)-like receptors (RLRs), nucleotide oligomerization domain-like receptors (NLRs), C-type lectins (CTLs), AIM2-like receptors (ALRs) and oligoadenylate synthase-like receptors (OLRs) (Thaiss et al., 2016). Among them, the RIG-I-like receptors, specifically MDA5 and RIG-I, act as the major cytoplasmic sensors for viral RNA and initiate the innate immune responses upon viral infection (Loo and Gale, 2011).

In 2002, MDA5 was first discovered in human melanoma cells (Kang et al., 2002). MDA5 is known to recognize relatively long double-stranded RNA (dsRNA). Previous studies have revealed that MDA5 recognizes RNA from viruses such as measles virus (MV) and poliovirus, thereby initiating the antiviral innate immune response (Abe et al., 2012; Kato et al., 2008; Takaki et al., 2011). The structure of MDA5 comprises two N-terminal caspase recruitment domains (CARDs), an RNA helicase domain, and a C-terminal domain (CTD) (Yoneyama et al., 2005). Upon infection, the CARDs of MDA5 interact with the CARD of the adaptor protein mitochondrial antiviral signaling protein (MAVS). This interaction leads to the recruitment of tank-binding kinase 1 (TBK1) and inhibitor of NF-κB (Nuclear factor kappa-B) kinase ε (IKKε) and then triggers the phosphorylation and nuclear translocation of interferon regulatory factor 3 and 7 (IRF3/7). Ultimately, the expression of type-I IFNs is activated (Honda et al., 2005; Rehwinkel and Reis e Sousa, 2010; Seth et al., 2005).

* Corresponding author.State Key Laboratory of Developmental Biology of Freshwater Fish, College of Life Science, Hunan Normal University, Changsha, 410081, China.

** Corresponding author.State Key Laboratory of Developmental Biology of Freshwater Fish, College of Life Science, Hunan Normal University, Changsha, 410081, China.

E-mail addresses: xiaojun2018@hunnu.edu.cn (J. Xiao), fenghao@hunnu.edu.cn (H. Feng).

https://doi.org/10.1016/j.dci.2023.105059
Received 29 July 2023; Received in revised form 12 September 2023; Accepted 12 September 2023
Available online 16 September 2023

Table 1
Primers used in this study.

Primer	Sequence (5′-3′)	Application
Vector Construction		
bcRIOK3-F	ACTGACGGTACCATGGACCAACTTGAAGT	pcDNA5/FRT/TO-Flag/HA/Myc-bcRIOK3 construction
bcRIOK3-R	ACTGACCTCGAGTTAATCATCATCAGTGT	
qRT-PCR		
Q-bcRIOK3-F	TGCTCTCTGGCTGATGTTAT	ex vivo qRT-PCR
Q-bcRIOK3-R	TAGGGGTAGTGGTTGGTTTG	
Q-SVCV-M-F	CGACCGCGCCAGTATTGATGGATAC	
Q-SVCV-M-R	ACAAGGCCGACCCGTCAACAGAG	
Q-SVCV-N-F	GGTGCGAGTAGAAGACATCCCCG	
Q-SVCV-N-R	GTAATTCCCATCATTGCCCCAGAC	
Q-SVCV-P-F	AACAGGTATCGACTATGGAAGAGC	
Q-SVCV-P-R	GATTCCTCTTCCCAATTGACTGTC	
Q-SVCV-G-F	GATGACTGGGAGTTAGATGGC	
Q-SVCV-G-R	ATGAGGGATAATATCGGCTTG	
Q-EPC actin-F	AAGGAGAAGCTCTGCTATGTGGCT	
Q-EPC actin-R	AAGGTGGTCTCATGGATACCGCAA	
Q-EPC IFN-F	ATGAAAACTCAAATGTGGACGTA	
Q-EPC IFN-R	GATAGTTTCCACCCATTTCCTTAA	
Q-EPC ISG15-F	TGATGCAAATGAGACCGTAGAT	
Q-EPC ISG15-R	CAGTTGTCTGCCGTTGTAAATC	
Q-EPC MX1-F	TGGAGGAACCTGCCTTAAATAC	
Q-EPC MX1-R	GTCTTTGCTGTTGTCAGAAGATTAG	
Q-EPC Viperin-F	ATGAAAACTCAAATGTGGACGTA	
Q-EPC Viperin-R	GATAGTTTCCACCCATTTCCTTAA	
shRNA		
sh-bcRIOK3-1-F	CCGGGGGATACTGGAGAGCATCAACGCTCGAGCGTTGATGCTCTCCAGTATCCTTTTTG	bcRIOK3 knockdown
sh-bcRIOK3-1-R	AATTCAAAAAGGATACTGGAGAGCATCAACGCTCGAGCGTTGATGCTCTCCAGTATCC	
sh-bcRIOK3-2-F	CCGGGGAGCTTTGAAGAGAAGATTGCTCGAGCAATCTTCTCTTCAAAGCTCCTTTTTG	
sh-bcRIOK3-2-R	AATTCAAAAAGGAGCTTTGAAGAGAAGATTGCTCGAGCAATCTTCTCTTCAAAGCTCC	
sh-bcRIOK3-3-F	CCGGGGCACAACCTCACCAGGATAAACTCGAGTTTATCCTGGTGAGGTTGTGCTTTTTG	
sh-bcRIOK3-3-R	AATTCAAAAAGCACAACCTCACCAGGATAAACTCGAGTTTATCCTGGTGAGGTTGTGC	

Table 2
Comparisons of bcRIOK3 with other vertebrate RIOK3 protein sequences (%).

Species	Full-length sequence		NCBI Accession	Species	Full-length sequence		NCBI Accession
	Identity	Similarity	Number		Identity	Similarity	Number
M.piceus	100.00	100.00	OR208546	*H.capensis*	77.60	85.74	XP_053105404.1
C.idella	98.22	98.61	XP_051738425.1	*L.chalumnae*	73.73	83.52	XP_005990813.1
L.rohita	93.47	96.23	KAI2648813.1	*M.monax*	73.80	82.85	KAI6061264.1
D.rerio	92.50	95.26	NP_001003614.1	*N.asiaeorientalis*	75.60	85.00	XP_024613662.1
I.punctatus	82.38	90.69	AHH38008.1	*D.leucas*	75.60	85.00	XP_022442534.1
E.lanceolatus	77.91	87.57	XP_033495152.1	*S.scrofa*	75.75	84.56	JAG69217.1
T.amazonica	77.25	89.41	XP_034041760.1	*M.musculus*	73.18	82.75	NP_077144.2
T.fulvidraco	79.41	88.31	XP_027017913.2	*L.weddellii*	73.41	83.23	XP_006734695.1
C.mydas	79.15	87.85	XP_007057070.2	*M.coucha*	73.89	82.97	XP_031220835.1
C.moneduloides	78.50	87.62	XP_031979432.1	*C.hircus*	73.41	82.65	XP_005697103.2
N.furzeri	75.39	86.61	XP_015830158.1	*M.mulatta*	75.00	84.80	XP_014977152.1
A.fuligula	78.74	87.44	XP_032038244.1	*M.fascicularis*	75.00	84.80	XP_045233898.1
A.platyrhynchos	78.38	87.47	XP_027307744.1	*M.auratus*	73.69	82.59	XP_005065437.1
C.porosus	77.46	86.92	XP_019402531.1	*B.taurus*	75.55	84.36	NP_001069304.1
T.bernacchii	75.39	84.76	XP_034003052.1	*O.anatinus*	75.40	83.80	XP_028924717.1
G.flavomarginatus	78.70	87.01	XP_050798832.1	*M.oregoni*	72.61	82.37	XP_041516238.1
G.gangeticus	77.46	86.51	XP_019381870.1	*E.caballus*	75.05	84.50	XP_005612823.1
R.bivittatum	77.76	87.14	XP_029446987.1	*H.sapiens*	74.60	84.20	AAH39729.1
G.gallus	77.94	86.43	XP_040521526.1	*R.norvegicus*	73.69	83.36	NP_001101893.1
G.seraphini	79.30	86.68	XP_033789769.1	*X.laevis*	72.08	83.36	NP_001087045.1
S.habroptila	77.55	86.73	XP_030361697.1	*R.roxellana*	74.90	84.93	XP_010381538.1
M.unicolor	78.25	86.38	XP_030069376.1	*O.hannah*	64.39	71.62	ETE68087.1
S.townsendi	76.92	86.23	XP_048364145.1				

Right open reading frame kinase 3 (RIOK3) is an atypical serine/threonine protein kinase, which belongs to the RIO family and is conserved in eukaryotes. RIO family includes RIO kinase 1 (RIOK1), RIO kinase 2 (RIOK2) and RIO kinase 3 (RIOK3) (Li et al., 2022; Wang et al., 2019b). It has been reported that RIOK3 is an oncogene in breast cancer, prostatic cancer, and pancreatic cancer through various regulatory mechanisms (Kimmelman et al., 2008; Mishra et al., 2010; Singleton et al., 2015). RIOK3 has also been identified as a component of cytoplasmic pre-40 S pre-ribosomal particles (Baumas et al., 2012). Besides, RIOK3 has been shown to regulate the type I IFN pathway during viral infection, although its regulation mechanism remains controversial in different studies. On the one hand, a group has reported that RIOK3

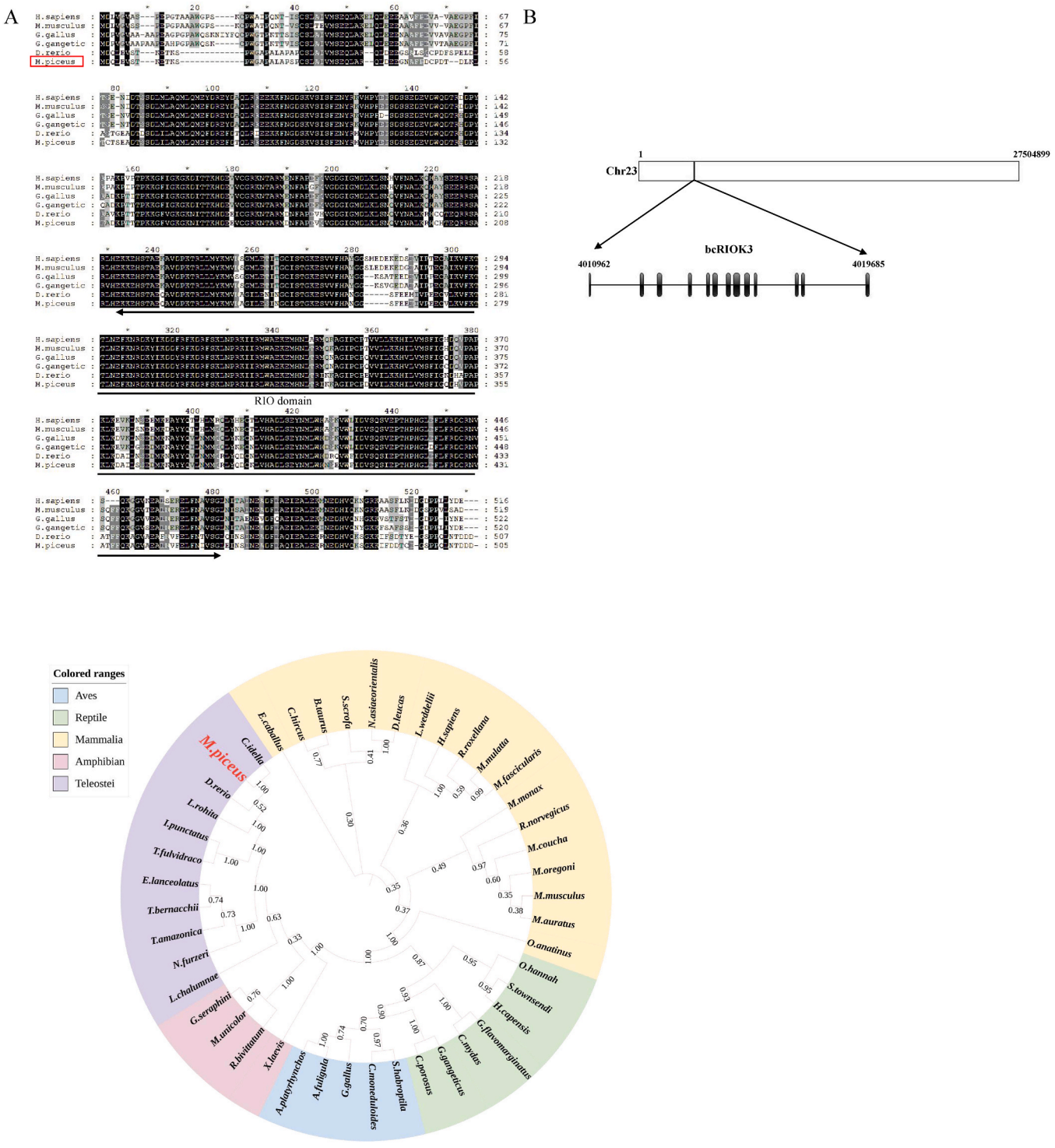

Fig. 1. Sequences analysis of bcRIOK3. (A) Multi-sequence alignment of RIOK3 from 6 species by GeneDoc, containing *H. sapiens* (AAH39729.1), *M. musculus* (NP_077144.2), *G. gallus* (XP_040521526.1), *G. gangeticus* (XP_019381870.1), *D. rerio* (NP_001003614.1) and *M. piceus* (OR208546). (B) The genomic information of bcRIOK3. The chromosome analysis map is done using the online tool IBS (http://ibs.biocuckoo.org/online.php#). (C) The phylogenetic tree was generated from RIOK3 sequences of 44 species using the neighbor-joining method of the MEGAX program (NCBI accession numbers were listed in Table 2) and was embellished via the online tool iTOL (https://itol.embl.de/). The numbers on the branches represent bootstraps.

physically bridges TBK1 and IRF3 to activate the IFN-β pathway upon viral infection in HEK293T cells (Feng et al., 2014). On the other hand, another group has demonstrated that in HEK293T cells, RIOK3 interacts with and phosphorylates MDA5 to weaken its assembly, and then attenuates the MDA5-mediated innate immune response (Takashima et al., 2015). Therefore, further investigation is required to determine the precise function and molecular mechanism of RIOK3 in regulating the type I IFN pathway.

In this study, a RIOK3 homolog of black carp (bcRIOK3) has been cloned and characterized. The results confirm the negative regulatory role of bcRIOK3 in the bcMDA5-mediated innate immune response. Specifically, overexpression of bcRIOK3 led to a suppression of bcMDA5-

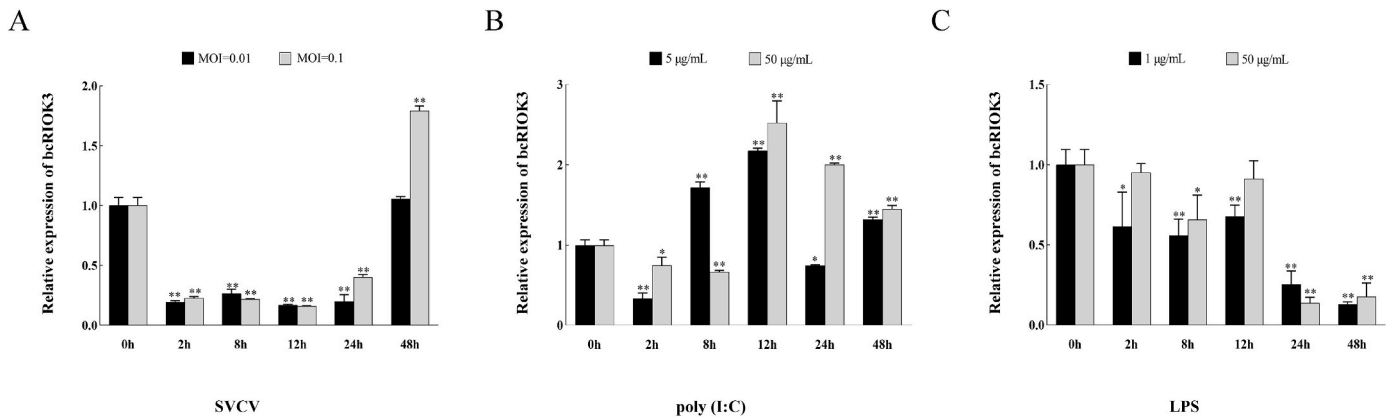

Fig. 2. The mRNA levels of bcRIOK3 in host cells under different stimuli. (A~C) MPK cells were infected with SVCV (MOI = 0.01 or MOI = 0.1) (A), treated with poly (I:C) (5 μg/mL or 50 μg/mL) (B), or stimulated with LPS (1 μg/mL or 50 μg/mL) (C), respectively. The cells were harvested at 0 h, 2 h, 8 h, 12 h, 24 h, and 48 h. The quantification analysis of mRNA levels of bcRIOK3 was determined by qRT-PCR. The error bar represents ±SD. The asterisk (* or **) stands for statistical difference (*$p < 0.05$, **$p < 0.01$).

mediated IFN promoter transcription and a reduction in bcMDA5-mediated antiviral activity. Mechanistically, bcRIOK3 interacted with bcMDA5 and enhanced the K48-linked ubiquitination of bcMDA5 and subsequently facilitated the degradation by proteasome pathway. Collectively, our data provide the first evidence in teleost fish that bcRIOK3 is a negative regulator of bcMDA5 in the host antiviral innate immune response.

2. Materials and methods

2.1. Cells and plasmids

HEK293T cells, HeLa cells, Epithelioma Papulosum Cyprinid (EPC) cells, and *Mylopharyngodon piceus* kidney (MPK) cells were kept in the laboratory and these cell lines were cultured in Dulbecco's modified Eagle's medium (DMEM) containing 10% fetal bovine serum (FBS), 2 mM L-glutamine, penicillin (100 U/mL) and streptomycin (100 mg/mL) (Zhou et al., 2015). EPC and MPK cells were cultured at 26 °C with 5% CO_2; HEK293T and HeLa cells were cultured at 37 °C with 5% CO_2.

pcDNA5/FRT/TO, pcDNA5/FRT/TO-HA-bcMDA5, pRL-TK, Luci-bcIFNa (for black carp IFNa promoter activity analysis), Luci-DrIFNφ1 (for zebrafish IFNφ1 promoter activity analysis) and Luci-epcIFN (for EPC IFN promoter activity analysis) were kept in the lab. The recombinant expression vector Flag-bcRIOK3 was constructed by inserting the open reading frame (ORF) of bcRIOK3 into pcDNA5/FRT/TO-Flag. The primers used in this study were referenced in Table 1.

2.2. Virus production and titration

Spring viremia of carp virus (SVCV, strain: SVCV741) was kept in the lab and produced in EPC cells at 26 °C in the presence of 2% FBS. Virus titers were determined via plaque assay on EPC cells (Wang et al., 2019a). Briefly, the gene was transfected into EPC cells via polyethylenimine (PEI). At 24 h post-transfection, EPC cells were infected with SVCV for 1 h, medium was removed and replaced with medium containing 2% FBS. After infection with SVCV 24 h, the viral supernatant was collected and the titer was measured using EPC cells. The viral supernatant was applied to 10-fold serial dilution and the array of the diluted virus was added to EPC cells. After 1 h incubation at 26 °C, the supernatant was changed with fresh DMEM containing 2% FBS and 1% methylcellulose. And the plaques were counted on day 3 post-infection.

2.3. LPS and poly (I:C) treatment

Lipopolysaccharide (LPS) and polyinosinic-polycytidylic acid (poly (I:C)) were used for the stimulation of MPK cells for different time periods (2 h, 8 h, 12 h, 24 h, and 48 h). LPS or poly (I:C) was dissolved in PBS and prepared at 10 mg/mL. LPS was added directly into the medium with a final concentration of 1 or 50 mg/mL separately; and poly (I:C) was directly added into the medium as well with a concentration of 5 or 50 mg/mL separately.

2.4. Quantitative real-time PCR (qRT-PCR)

Quantitative real-time PCR was performed to detect the relative mRNA level of genes, including bcRIOK3, SVCV encoding genes (M, N, P, G), IFN, and interferon-stimulated genes (*ISG15*, *MX1*, and *Viperin*) in the SVCV-infected cells. The primer sequences for qRT-PCR were listed in Table 1. The qRT-PCR program was: 1 cycle of 95 °C/10 min, 40 cycles of 95 °C/15 s, 60 °C/1 min. The data was calculated by the $2^{-\Delta\Delta CT}$ method as previously described (Wang et al., 2021).

2.5. Immunoblotting (IB)

Immunoblotting was used to detect the expression of target proteins in EPC cells and HEK293T cells. The cells were harvested at 48 h post-transfection (hpt), and total proteins were extracted by lysing EPC or HEK293T in lysis buffer (50 mM Tris-HCl, 150 mM NaCl, 5 mM EDTA, 1% NP-40, pH 7.4). The lysed cells were separated by 10% SDS-PAGE and transferred to PVDF membranes. Then the membranes were incubated with the primary antibodies after blocking with 5% non-fat milk in TBS overnight. After 4 times of wash with TBST (0.1% Tween-20 in TBS), the membranes were incubated with the secondary antibodies. Finally, the target proteins on the PVDF membranes were visualized by BCIP/NBT Alkaline Phosphatase Color Development Kit (Thermo, USA).

2.6. Immunofluorescence microscopy

HeLa cells in a 24-well plate were transfected with bcRIOK3 (300 ng/well) and bcMDA5 (300 ng/well) by using Lipomax (SUDGEN, China). The transfected HeLa cells were fixed with 4% (v/v) paraformaldehyde for 15 min and permeabilizated with Triton X-100 (0.2% in PBS) for 15 min. Then the cells were blocked with 10% goat serum (Solarbio, China) for 1 h. Afterward, the cells were incubated with anti-Flag antibody or anti-HA antibody at the ratio of 1:500. After six times of wash with PBS, the cells were incubated with the secondary antibodies, containing Alexa 594 and Alexa 488 at the ratio of 1:1000. After six times of wash with PBS, DAPI was used for nuclear staining. Eventually, the cells were photographed using a confocal microscope (Olympus, Japan) (Yang et al., 2019).

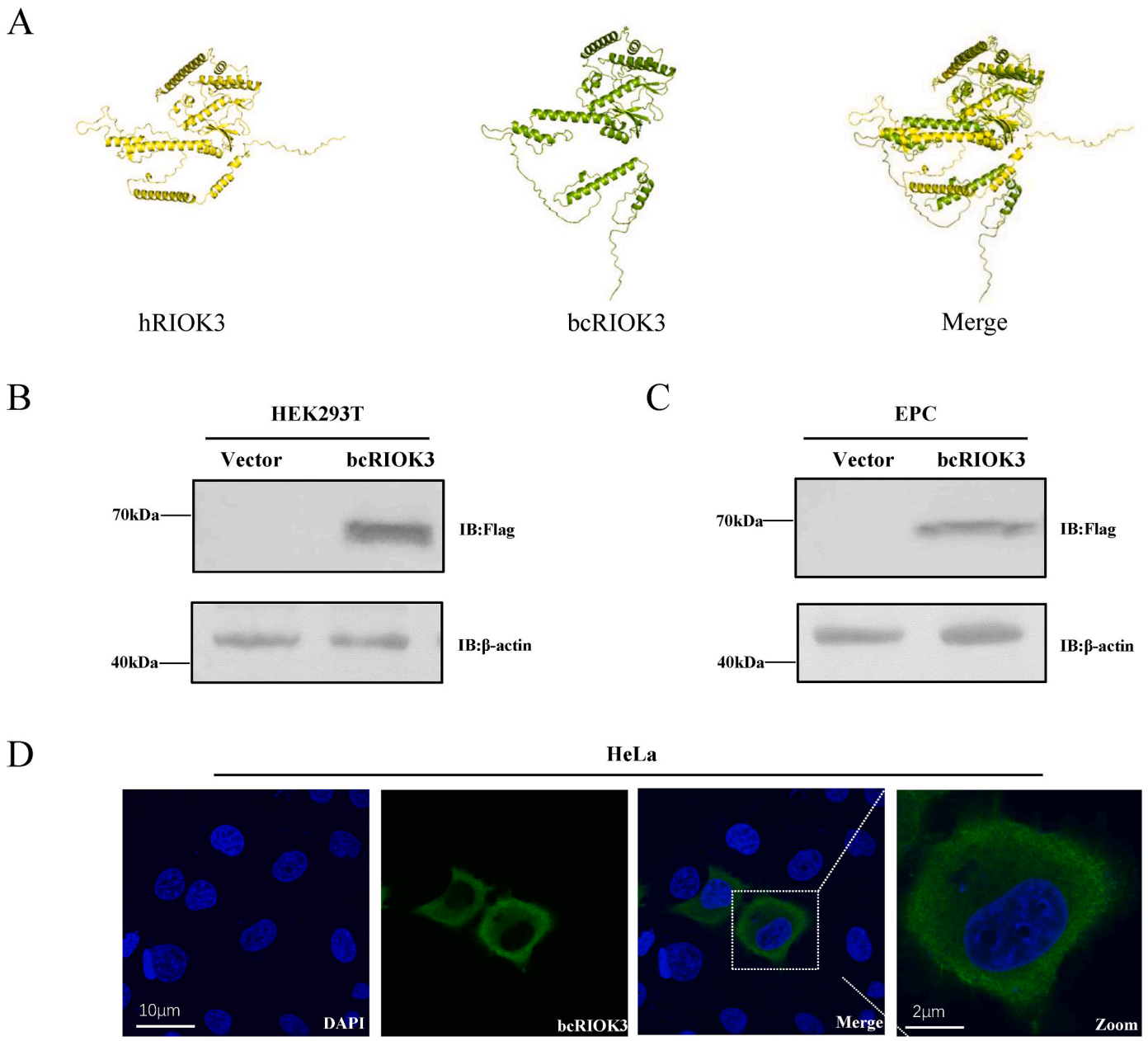

Fig. 3. The predicted structure, expression, and subcellular distribution of bcRIOK3 protein. (A) Three-dimensional structure prediction of human RIOK3 (hRIOK3) and bcRIOK3 were predicted by online tools: alphafold and alphafold2, respectively. The protein structure of hRIOK3 and bcRIOK3 were merged by PyMOL. (B) & (C) Immunoblot assay of bcRIOK3 in HEK293T cells and EPC cells. HEK293T cells and EPC cells in 6-well plates were transfected with empty vector (3 μg/well) or Flag-bcRIOK3 (3 μg/well). At 48 h post-transfection, cells were collected for IB assay. (D) HeLa cells in 24-well plates were transfected with Flag-bcRIOK3 and cells were subjected to immunofluorescence staining at 24 h post-transfection. IB: Immunoblot. Vector: pcDNA5/FRT/TO-Flag. bcRIOK3: pcDNA5/FRT/TO-Flag-bcRIOK3. The scales represented 10 μm or 2 μm.

2.7. Luciferase reporter assay

To detect the effect of bcRIOK3 on bcMDA5-mediated IFN promoter transcription, bcRIOK3 was dose-dependent co-transfected into EPC cells in 24-well plates with bcMDA5, pRL-TK, and Luci-bcIFNa (-DrIFNφ1 or -epcIFN) for 24 h (the black carp interferon (bcIFNa), EPC interferon (epcIFN) and zebrafish interferon 1 (DrIFNφ1) were all type I interferon). Then the cells were collected and lysed by passive lysis buffer (PLB) for 15 min at ice. The centrifuged supernatant was used to measure the activities of firefly luciferase and renilla luciferase according to the manufacturer's protocol (Promega, USA) (Wang et al., 2021).

2.8. Co-immunoprecipitation (co-IP)

HEK293T cells in the 10 cm dish were co-transfected with pcDNA5/FRT/TO-HA-bcMDA5 and pcDNA5/FRT/TO-Flag-bcRIOK3 (or empty vector) separately. co-IP were performed at 48 hpt as previously described (Wang et al., 2021). The whole cell lysate of the transfected cells was incubated with protein A/G agarose beads at 4 °C for 1 h. After precleaning and concentration, the anti-Flag conjugated protein A/G agarose beads were added and incubated with the supernatant media at 4 °C for overnight. After 4 times of washing with 1% NP-40 buffer, the beads were boiled in 5 × sample buffer and used for IB assay as above described.

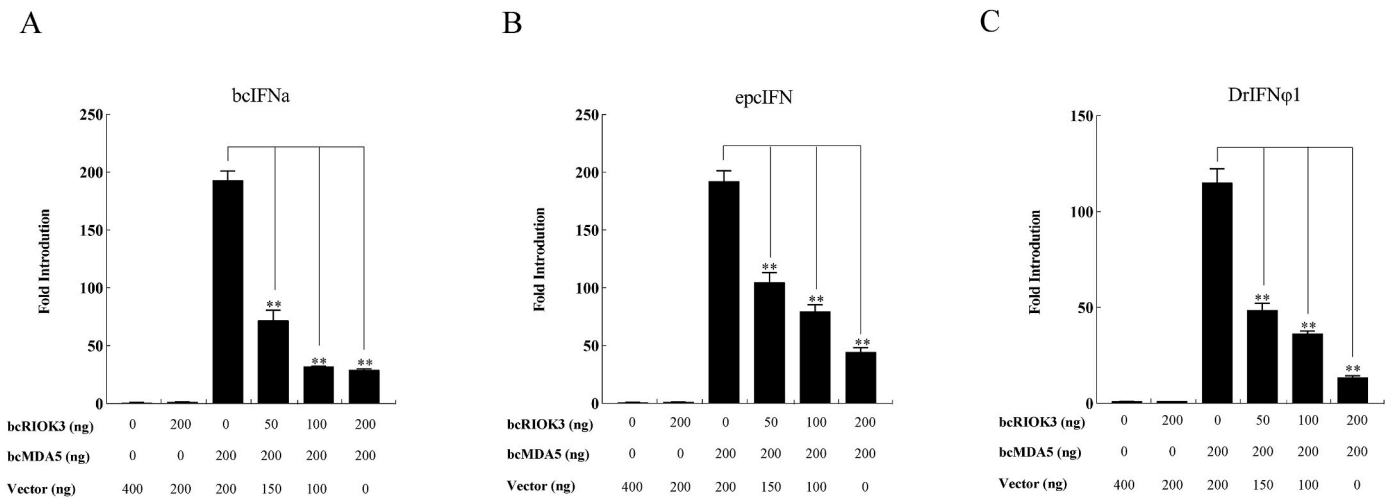

Fig. 4. bcRIOK3 inhibits the bcMDA5-mediated activation of interferon promoters. (A~C) The reporter plasmid pRL-TK, Luci-bcIFNa (A), Luci-epcIFN (B), or Luci-DrIFNφ1 (C) were co-transfected into EPC cells with the indicated doses of plasmids bcRIOK3 and bcMDA5 into EPC cells, respectively. The total amount of plasmids in each well is 625 ng. The transcription activities of IFN promoters were detected by the luciferase reporter assay 24 h after transfection. The error bar represents ±SD. The number above the error bar stands for the average IFN fold induction. bcRIOK3: pcDNA5/FRT/TO-Flag-bcRIOK3. bcMDA5: pcDNA5/FRT/TO-HA-bcMDA5. Vector: pcDNA5/FRT/TO. *$p < 0.05$, **$p < 0.01$.

2.9. shRNA design

To construct bcRIOK3 shRNA oligonucleotides, per pairs of shRNA oligos (listed in Table 1) targeting the CDS of bcRIOK3 gene were designed according to the online tool BLOCK-iT™ RNAi Designer (http://rnaidesigner.thermofisher.com/rnaiexpress). The bcRIOK3 shRNA plasmids, including pLKO-shRNA-bcRIOK3-1, pLKO-shRNA-bcRIOK3-2 and pLKO-shRNA-bcRIOK3-3 were inserted into pLKO.1TRC.

2.10. Semi-denaturing detergent agarose gel electrophoresis (SDD-AGE)

HEK293T cells in a 10 cm dish were transfected with pcDNA5/FRT/TO-Flag-bcRIOK3, pcDNA5/FRT/TO-HA-bcMDA5, or empty vector, separately. Then the co-IP assay was performed as above described. After 4 times of washing with 1% NP-40 buffer, add 40 μL 1% NP40 lysate and 1 μL HA peptide to the tube, bounce on ice for 30 min, and put on ice for 2 h. Then, samples were centrifuged at 3000 rpm for 2 min and transferred the eluate to a new 1.5 mL EP tube. Subsequently, the 4 × loading buffer was added to the samples and performed SDD-AGE electrophoresis (Halfmann and Lindquist, 2008).

2.11. Statistics analysis

For the statistical analysis, all the data were conducted in triplicate. Error bars represent the standard error of the mean (+SEM) of three independent experiments. The data from three independent experiments were analyzed by the two-tailed student's t-test. An asterisk (*) stands for $p < 0.05$ and is considered the statistics were significant, two asterisks (**) stand for $p < 0.01$ and are considered the statistics were highly significant.

3. Results

3.1. Sequence analysis of bcRIOK3

To study the function of RIOK3 in teleost, we cloned the full-length CDS of bcRIOK3 from the black carp spleen and constructed the plasmids with different tags. The sequence analysis results demonstrated that bcRIOK3 (NCBI accession number: OR208546) contains 1518 nucleotides and encodes 506 amino acids (Supplementary Fig. 1). The predicted molecular mass and the theoretical isoelectric of bcRIOK3 are 57.7 kDa and 5.44, respectively (calculated by EXPASy Compute PI/Mw). To investigate the conservation of bcRIOK3 in evolution, the amino acid sequence of bcRIOK3 was aligned with that of other homologous proteins, including RIOK3 of human (*Homo sapiens*), mouse (*Mus musculus*), chicken (*Gallus gallus*), gharial (*Gavialis gangeticus*) and zebrafish (*Danio rerio*). The alignment results showed that the sequence of bcRIOK3 is conserved in different species, especially the RIO domain (amino acids 212 to 455) (Fig. 1A). By analyzing the genome information of black carp, we found that the bcRIOK3 gene is located on chromosome 23 and composed of 13 exons (Fig. 1B). Furthermore, the phylogenetic tree was constructed based on the nucleotide sequences of RIOK3 from different vertebrates, showing that bcRIOK3 clusters tightly with *Ctenopharygodon Idella* RIOK3 (Fig. 1C).

3.2. In vitro expression of bcRIOK3 in response to different stimulation

In order to study the function of bcRIOK3 in the host's innate immune response, we treated MPK cells with SVCV, poly (I:C), and LPS. Subsequently, we detected the mRNA expression level of bcRIOK3 in the host cell using qRT-PCR. When cells were infected with SVCV, the mRNA expression level of bcRIOK3 was initially low in both groups (MOI = 0.01&MOI = 0.1) during the pre-infection period. However, at 48 h post-infection (hpi), the expression level of bcRIOK3 significantly increased in the high MOI group (MOI = 0.1) (Fig. 2A). Following stimulation with poly (I:C), the mRNA levels of bcRIOK3 in both groups (5 μg/mL&50 μg/mL) decreased and then increased, and the mRNA levels of bcRIOK3 reached a maximum at 12 hpi (5 μg/mL, 2.2 folds; 50 μg/mL, 2.5 folds) (Fig. 2B). After LPS treatment, the mRNA levels of bcRIOK3 showed a decreasing trend, suggesting that bcRIOK3 may be involved in the host cell's antibacterial immune response (Fig. 2C). In summary, these data demonstrate that bcRIOK3 is probably involved in the antiviral and antibacterial immune response of black carp.

3.3. The protein structure, expression, and subcellular localization of bcRIOK3

The protein structure of human (hRIOK3) and bcRIOK3 were predicted individually using alphafold (https://alphafold.com/) and alphafold2 (https://colab.research.google.com/github/deepmind/alphafold/blob/main/notebooks/AlphaFold.ipynb) and the protein structure of hRIOK3 and bcRIOK3 were merged using the software PyMOL.

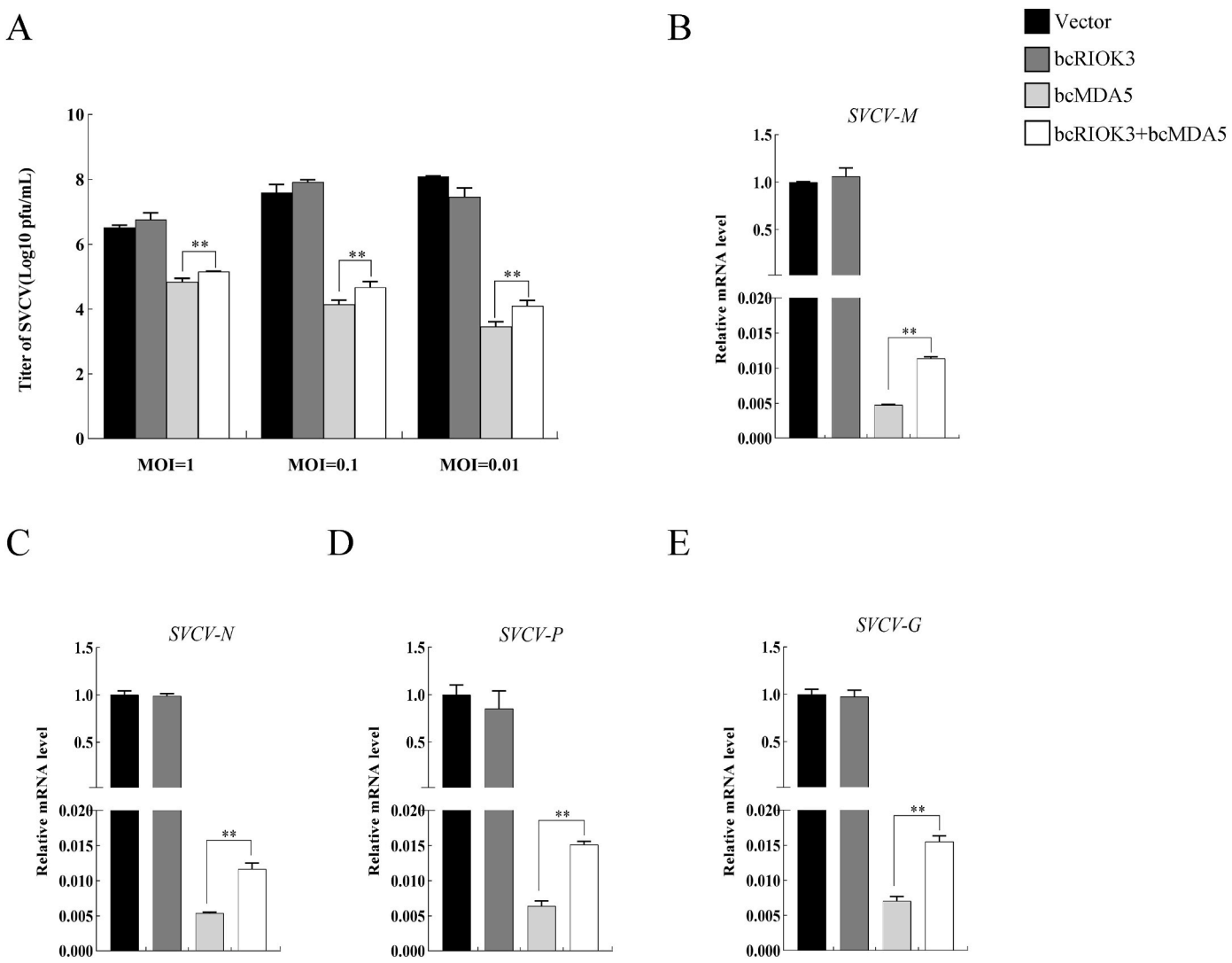

Fig. 5. bcRIOK3 inhibits bcMDA5-mediated antiviral activity. (A) EPC cells in 24-well plates were transfected with bcRIOK3, bcMDA5 or co-transfected with bcRIOK3 and bcMDA5. The total amount of plasmids in each well is 400 ng. The transfected cells were infected with SVCV at MOI of 1, 0.1, and 0.01 respectively. The viral supernatant was harvested at 24 h post-infection (hpi) for virus titers measurement. (B ~ E) EPC cells in 6-well plates were transfected with bcRIOK3, bcMDA5 or co-transfected with bcRIOK3 and bcMDA5 respectively. The total amount of plasmids in each well is 3 μg. Then, the transfected cells were infected with SVCV at MOI of 0.1. The cells were collected and used for RNA isolation at 24 hpi. The relative mRNA level of SVCV-M (B), SVCV-N (C), SVCV-P (D), and SVCV-G (E) were examined by qRT-PCR. bcRIOK3: pcDNA5/FRT/TO/Flag-bcRIOK3. bcMDA5: pcDNA5/FRT/TO/HA-bcMDA5. Vector: pcDNA5/FRT/TO. The error bar represents ±SD. *$p < 0.05$, **$p < 0.01$.

The results suggested that the protein structures between bcRIOK3 and hRIOK3 were similar at the C-terminus but differ at the N-terminus, which was consistent with the similarity of their amino acid sequence alignment (Fig. 3A). In order to verify the expression of bcRIOK3, we overexpressed bcRIOK3 with a Flag tag in HEK293T cells and EPC cells, respectively. The protein expression of bcRIOK3 was analyzed by western blotting assay. Specific bands of approximately 60 kDa were detected in both cells overexpressing bcRIOK3, while no specific bands were detected in the control group, indicating that bcRIOK3 was successfully expressed (Fig. 3B&C). Subsequently, we transfected HeLa cells with Flag-bcRIOK3 and assessed the subcellular localization of bcRIOK3 by immunofluorescence assay. The results showed that bcRIOK3, visualized as green fluorescence, wrapped around the nucleus labeled with blue fluorescence, indicating that bcRIOK3 is mainly distributed in the cytoplasm (Fig. 3D).

3.4. bcRIOK3 restricted bcMDA5 mediated interferon production

To investigate the function of bcRIOK3 in the IFN signaling pathway, we transfected bcRIOK3 and/or bcMDA5 into EPC cells for luciferase reporter assay. The results showed that bcMDA5 significantly activated the type I IFN promoters: 193.2-fold for bcIFNa (Fig. 4A), 192.4-fold for epcIFN (Figs. 4B), and 115.1-fold for DrIFNφ1 (Fig. 4C) while bcRIOK3 did not activate the promoters. However, we found that bcRIOK3 inhibited the ability of bcMDA5 to activate bcIFNa, epcIFN, and DrIFNφ1 promoters in a dose-dependent manner (Fig. 4ÃC). In a word, these results suggested that bcRIOK3 inhibited bcMDA5-mediated interferon production.

3.5. bcRIOK3 suppressed bcMDA5-mediated antiviral activity

To further investigate the role of bcRIOK3 in the innate antiviral immunity of black carp, we co-transfected bcRIOK3 and/or bcMDA5 into EPC cells for SVCV infection. At 24 hpi, the SVCV-infected cells with different MOIs (MOI = 1, MOI = 0.1, and MOI = 0.01) were collected to determine their viral titers. The results showed that bcMDA5 significantly inhibited SVCV replication in EPC cells. However, the viral titers of the supernatants in cells co-expressing bcRIOK3 and bcMDA5 were

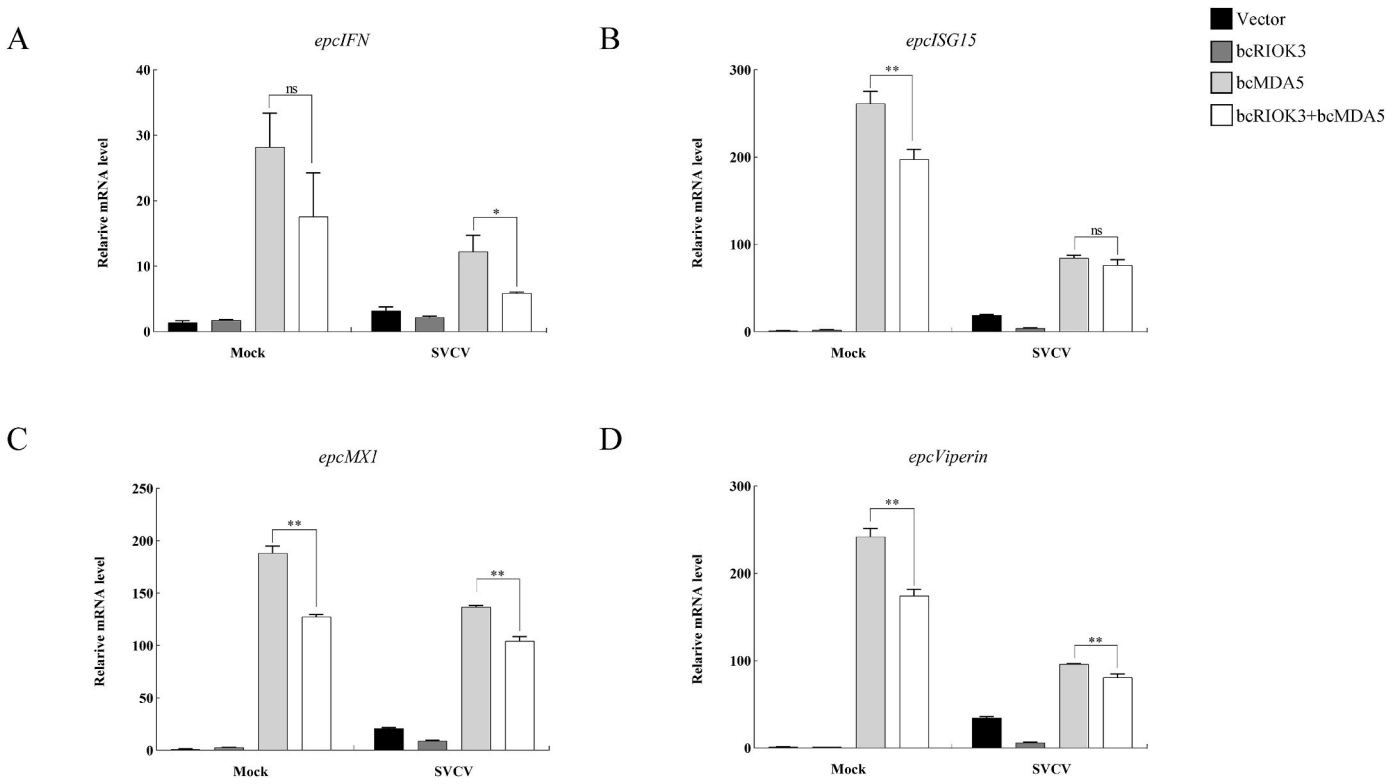

Fig. 6. bcRIOK3 inhibits the mRNA levels of IFN and ISGs in EPC cells with/without SVCV infection. (A~D) EPC cells in 6-well plates were transfected with bcRIOK3, bcMDA5 or co-transfected with bcRIOK3 and bcMDA5 respectively. The total amount of plasmids in each well is 3 μg. Twenty-four hours post-transfection, cells were infected with SVCV at MOI of 0.1 or left untreated (Mock). Another 24 h later, the cells were collected and used for RNA isolation at 24 hpi. The relative mRNA level of *epcIFN* (A), *epcISG15* (B), *epcMX1* (C), and *epcViperin* (D) were examined by qRT-PCR, respectively. bcRIOK3: pcDNA5/FRT/TO/Flag-bcRIOK3. bcMDA5: pcDNA5/FRT/TO/HA-bcMDA5. Vector: pcDNA5/FRT/TO. The error bar represents ±SD. *$p < 0.05$, **$p < 0.01$.

higher than those of cells expressing bcMDA5 alone (Fig. 5A), indicating that bcRIOK3 inhibited bcMDA5-mediated antiviral activity. In addition, we examined the mRNA levels of SVCV-encoding genes in the SVCV (MOI = 0.1) infected group by qRT-PCR. The results showed that the mRNA levels of SVCV M (Fig. 5B), N (Fig. 5C), P (Fig. 5D), and G (Fig. 5E) in the bcRIOK3 and bcMDA5 co-transfected groups were significantly higher than those in the control group, which were consistent with the results of viral titer measurement. Furthermore, we detected the mRNA levels of *epcIFN*, *epcISG15*, *epcMX1*, and *epcViperin* in EPC cells by qRT-PCR. The results showed that the mRNA levels of *epcIFN* (Fig. 6A), *epcISG15* (Fig. 6B), *epcMX1* (Fig. 6C), and *epcViperin* (Fig. 6D) in EPC cells co-transfected with bcRIOK3 and bcMDA5 were reduced to different degrees before and after SVCV infection. In a word, these data demonstrated that bcRIOK3 prominently inhibits the bcMDA5-mediated interferon signaling pathway and antiviral activity.

3.6. Knockdown of bcRIOK3 potentiated the antiviral capacity of host cells

To study the role of bcRIOK3 in antiviral signaling in host cells, we designed shRNA to knock down bcRIOK3 in MPK cells. The knockdown efficiency was analyzed separately by IB and qRT-PCR assays. The IB results showed that co-transfection of bcRIOK3 with sh-bcRIOK3-3 in HEK293T cells led to a 70% reduction in exogenous bcRIOK3 protein levels (Fig. 7A). Besides, the qRT-PCR results showed that sh-bcRIOK3-3 also significantly reduced endogenous bcRIOK3 mRNA expression levels in MPK cells (Fig. 7A). Subsequently, MPK cells were transfected with sh-bcRIOK3-3 or scramble shRNA and infected with SVCV at MOI of 0.1. The results in Fig. 7B showed that the bcRIOK3 knockdown group exhibited significantly lower viral titer and reduced mRNA levels of SVCV-encoding genes compared to the control groups. Additionally, the transcription levels of the IFN-related genes, including *bcIFNa*, *bcIFNb* and *bcViperin* were observed to be higher in the bcRIOK3 knockdown group than those in the control groups after viral infection, but the basal mRNA levels of the above genes were decreased (Fig. 7C). In conclusion, the above results suggest that the knockdown of bcRIOK3 enhances the antiviral ability of host cells further confirming the negative regulatory role of bcRIOK3 in the host antiviral responses.

3.7. bcRIOK3 interacted with bcMDA5

To further study the interaction between bcRIOK3 and bcMDA5, we conducted a co-IP assay in HEK293T cells. The results showed that the specific band of HA-bcMDA5 was detected in the precipitated protein from Flag-bcRIOK3, while it was not detected in the control group, indicating that bcRIOK3 interacted with bcMDA5 (Fig. 8A). In addition, we performed an immunofluorescence assay in HeLa cells. The results showed considerable overlap in the subcellular localization of bcRIOK3 (green fluorescence) and bcMDA5 (red fluorescence) (Fig. 8B). These observations support the interaction between bcRIOK3 and bcMDA5.

3.8. bcRIOK3 reduced the oligomerization of bcMDA5 induced by poly (I:C)

The above data have demonstrated the negative regulatory effect of bcRIOK3 on bcMDA5, while the mechanism is unclear. According to previous research, MDA5 activates the antiviral immune response after recognizing RNA and undergoing multiple conformational changes (Bruns and Horvath, 2015). Upon recognition of cytoplasmic viral RNA, MDA5 initially binds to dsRNA in monomer form and then assembles into aggregates to bind with MAVS and activate the RLR downstream signaling pathway (Hou et al., 2011; Patel and García-Sastre, 2014; Xu

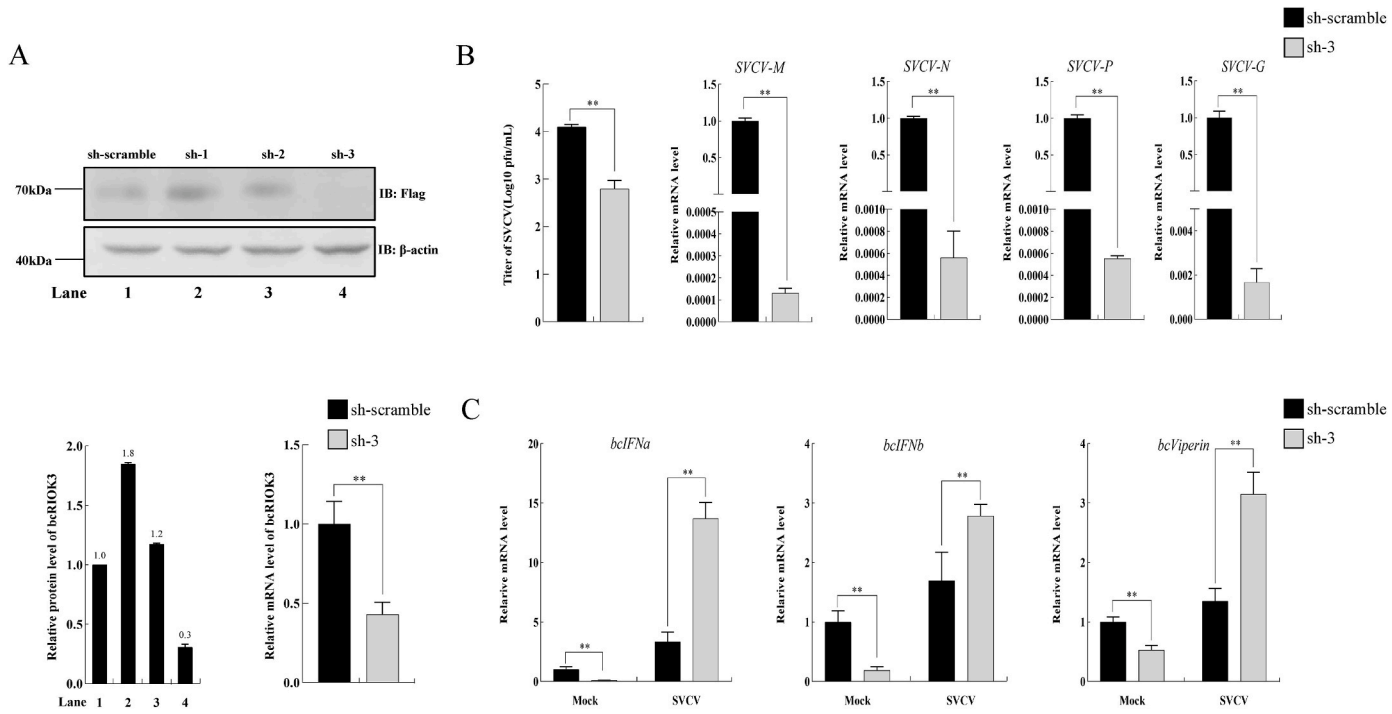

Fig. 7. Knockdown of bcRIOK3 enhances the antiviral capacity of host cells. (A) bcRIOK3 and shbcRIOK3 (or scramble shRNA) were co-transfected into HEK293T cells in 6-well plates, respectively. The expression level of bcRIOK3 was detected by immunoblot (IB) assay. The protein expression levels of bcRIOK3 were quantified using ImageJ software and normalized to β-actin. Then calculate the protein levels of each group relative to the scramble group (as control). Besides, MPK cells in a medium dish were transfected with scramble or sh-bcRIOK3-3. Then, the endogenous mRNA level of bcRIOK3 in MPK cells was detected by qRT-PCR. (B & C) MPK cells in a medium dish were transfected with scramble or sh-bcRIOK3-3. Twenty-four hours later, the cells were infected with SVCV at MOI of 0.1 for 24 h. Then, the supernatant was collected for viral titer assay and the infected MPK cells were harvested to detect the mRNA levels of the indicated genes by qRT-PCR. bcRIOK3: pcDNA5/FRT/TO/Flag-bcRIOK3. shbcRIOK3-1/2/3: pLKO-shRNA-bcRIOK3-1/2/3. Scramble: pLKO-shRNA-scramble. The error bar represents ±SD. ns: no significance, *P < 0.05, **P < 0.01.

et al., 2014). However, it has not been reported whether piscine MDA5 undergoes oligomerization. To study this, we transfected bcMDA5 into HEK293T cells, stimulated the cells with or without poly (I: C), and then performed semi-denaturing detergent agarose gel electrophoresis (SDD-AGE) assay. As shown in Fig. 9A, we found that bcMDA5 can undergo oligomerization without stimulation. Interestingly, after poly (I:C) stimulation, the oligomerization level of bcMDA5 increased. Furthermore, we explored whether bcRIOK3 affects the oligomerization of bcMDA5. The results in Fig. 9B showed that bcRIOK3 did not affect the oligomerization of bcMDA5 in the absence of poly (I: C) stimulation. However, in the presence of poly (I: C) stimulation, bcRIOK3 reduced the oligomerization of bcMDA5.

3.9. bcRIOK3 facilitated the ubiquitination and degradation of bcMDA5

We next investigated whether bcRIOK3 suppresses the function of bcMDA5 by inhibiting its protein expression. We co-transfected bcMDA5 with different doses of bcRIOK3 into HEK293T cells and harvested the cells at 48 hpt for western blotting. The results showed that the protein level of bcMDA5 decreased significantly with the increasing transfection dose of bcRIOK3, implying that bcRIOK3 might trigger the degradation of bcMDA5 (Fig. 10A). There were two major protein degradation pathways in the cells: the lysosomal pathway and the ubiquitin-proteasome pathway (Paudel et al., 2023). To explore the mechanism of bcRIOK3 inducing bcMDA5 protein degradation, we co-transfected bcRIOK3 and bcMDA5 into HEK293T cells and treated the cells with either the proteasome inhibitor MG132 or the lysosomal inhibitor chloroquine (CQ). The WB results showed that MG132 blocked the bcRIOK3-induced reduction in bcMDA5 protein levels (Fig. 10B), while CQ had no effect (Supplementary Fig. 2) indicating that bcRIOK3 triggers the protein degradation of bcMDA5 through the proteasome pathway. Furthermore, we co-transfected Myc-Ub, HA-bcMDA5, and Flag-bcRIOK3 into HEK293T cells and performed IP assays to assess the ubiquitination of bcMDA5. The results demonstrated that the ubiquitination of bcMDA5 in the bcMDA5 and bcRIOK3 co-transfection group was significantly higher than that in the bcMDA5 single-transfection group (Fig. 10C). In addition, to determine the linkage type of the ubiquitin chain of bcMDA5 regulated by bcRIOK3, we co-transfected HA-Ub, HA-Ub-K48O (or HA-Ub-K63O) with Flag-bcMDA5 and Myc-bcRIOK3 into HEK293T cells, respectively. The results revealed the K63-linked ubiquitination of bcMDA5 did not change significantly. However, the K48-linked ubiquitination of bcMDA5 in the co-transfection group was notably higher than that in the bcMDA5 single-transfection group (Fig. 10D). In summary, the results indicate that bcRIOK3 enhanced the K48-linked ubiquitination of bcMDA5 and facilitated the proteasome-dependent degradation of bcMDA5.

4. Discussion

Whether in mammals or fish, MDA5 is an important pattern recognition receptor for recognizing viral RNA (Andrejeva et al., 2004; Kang et al., 2002; Rothenfusser et al., 2005; Yoneyama et al., 2004, 2005). The regulation of MDA5 is essential for maintaining host immune homeostasis. In teleost, many molecules have been reported to regulate the function of MDA5. For instance, NAK-associated protein 1 (NAP1) and laboratory of genetics and physiology-2 (LGP2) positively regulate MDA5-mediated antiviral signaling during the innate immune activation in black carp (Cai et al., 2020; Liu et al., 2017). Similarly, zebrafish NOD1 can significantly strengthen the association between MDA5a and MAVS and acts as a positive modulator in MDA5/MAVS/IFN signaling (Wu et al., 2020). Besides, black carp dihydroxyacetone kinase (DAK) attenuates MDA5-mediated signaling in antiviral innate immunity (Liao

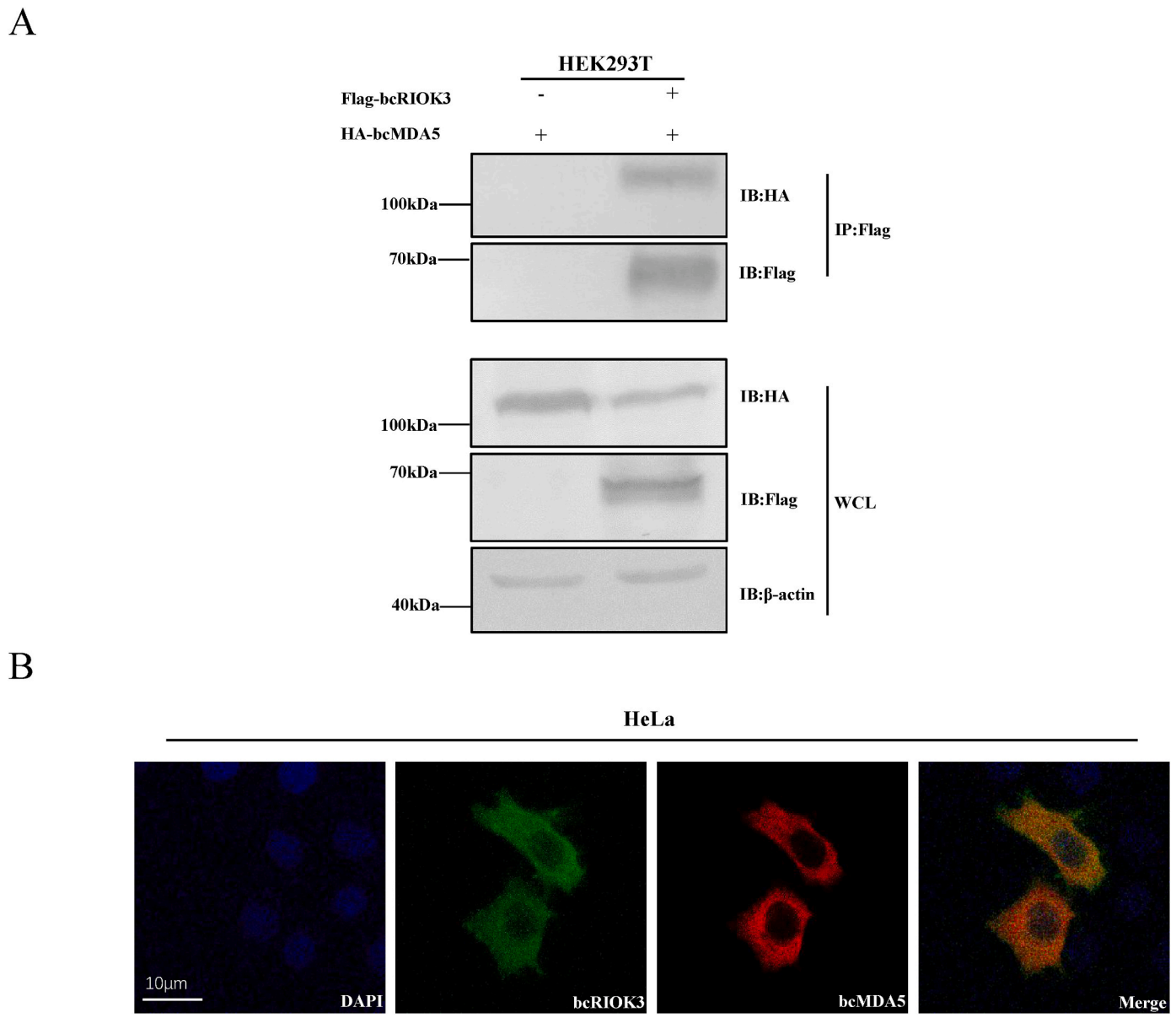

Fig. 8. The interaction and subcellular co-localization between bcRIOK3 and bcMDA5. (A) HEK293T cells in 10 cm plates were transfected with 7.5 μg bcMDA5 and 7.5 μg empty vector (or 7.5 μg bcRIOK3). At 48 h post-transfection, cells were harvested for co-IP assay. (B) HeLa cells in 24-well plates were transfected with 300 ng bcRIOK3 and 300 ng bcMDA5. Twenty-four hours later, cells were used for immunofluorescence assay. bcRIOK3: pcDNA5/FRT/TO/Flag-bcRIOK3. bcMDA5: pcDNA5/FRT/TO/HA-bcMDA5. Vector: pcDNA5/FRT/TO. IP: immunoprecipitation. IB: immunoblotting. WCL: whole cell lysate.

et al., 2022). Additionally, the tripartite motif 13 (TRIM13) negatively regulates MDA5-mediated antiviral response in orange-spotted grouper (Huang et al., 2016). However, there are no reports on the regulation of MDA5 by RIOK3 in teleost. In this paper, we identified that bcRIOK3 negatively regulates bcMDA5-mediated innate antiviral immune response.

In mammals, RIOK3 acts as an oncogene in a series of cancers such as breast cancer and prostate cancer, while also playing a role in the regulation of IFN signaling (Feng et al., 2014; Mishra et al., 2010; Singleton et al., 2015). The function of mammalian RIOK3 on IFN signaling regulation is controversial, exhibiting positive or negative regulatory effects. One group reported that RIOK3 physically bridges TBK1 and IRF3, thereby activating the downstream IFN-β pathway upon stimulation by several viruses and poly (I:C) (Feng et al., 2014). On the contrary, another group showed that RIOK3 interacts and phosphorylates MDA5 to damage its assembly, leading to the attenuation of SeV and poly (I:C)-induced innate immune response (Takashima et al., 2015). Interestingly, in this study, we found that, in the absence of viral infection, knocking down bcRIOK3 resulted in a decrease in the basal mRNA levels of IFN-related genes, including *bcIFNa*, *bcIFNb*, and *bcViperin* (the mock groups in Fig. 7C). However, it triggered significantly higher mRNA levels of these genes after viral infection (the SVCV groups in Fig. 7C). According to the findings in mammals, we hypothesized that in the resting state, bcRIOK3 may primarily function by targeting other molecules, such as TBK1 or IRF3, to positively regulate the IFN pathway. Therefore, knocking down bcRIOK3 leads to a decrease in the expression of the IFN-related genes. However, when cells are infected with the viruses or when MDA5 is activated, the primary function of bcRIOK3 is to bind to MDA5 and negatively regulate its function for avoiding excessive immune activation. Thus, in this condition, the knockdown of bcRIOK3 leads to the upregulation of ISG gene expression. In addition, since RIOK3 acts as a protein kinase rather than a ubiquitin ligase, the identification of the specific E3 ubiquitin ligase responsible for mediating bcMDA5 degradation will be worth exploring in our ongoing research.

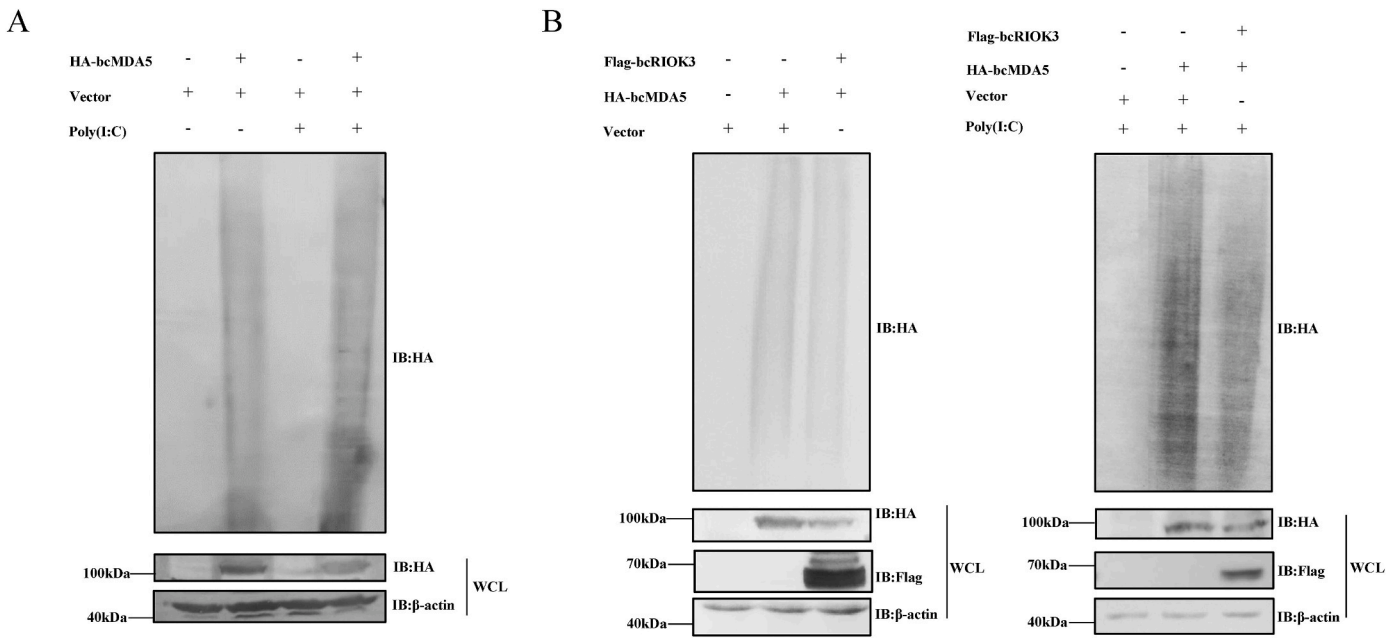

Fig. 9. The effect of bcRIOK3 on bcMDA5 oligomerization. (A) HEK293T cells in 10 cm plates were transfected with 7 μg HA-bcMDA5 and 7 μg empty vector (the cells transfected with 14 μg empty vector were used as the negative control). At 24 h after transfection, the experimental group cells were transfected with poly (I:C) (0.5 μg/mL). And 24 h later, the cells were collected for SDD-AGE. (B) HEK293T cells in 10 cm plates were transfected with 7.5 μg HA-bcMDA5 and 7.5 μg Flag-bcRIOK3 (or 7.5 μg empty vector). At 24 h after transfection, the experimental group cells were transfected with poly (I:C) (0.5 μg/mL). And 24 h later, the cells were collected for SDD-AGE. HA-bcMDA5: pcDNA5/FRT/TO/HA-bcMDA5. Flag-bcRIOK3: pcDNA5/FRT/TO/Flag-bcRIOK3. SDD-AGE: semi-denaturing detergent agarose gel electrophoresis. IB: immunoblotting. WCL: whole cell lysate. The error bar represents ±SD. **P < 0.01.

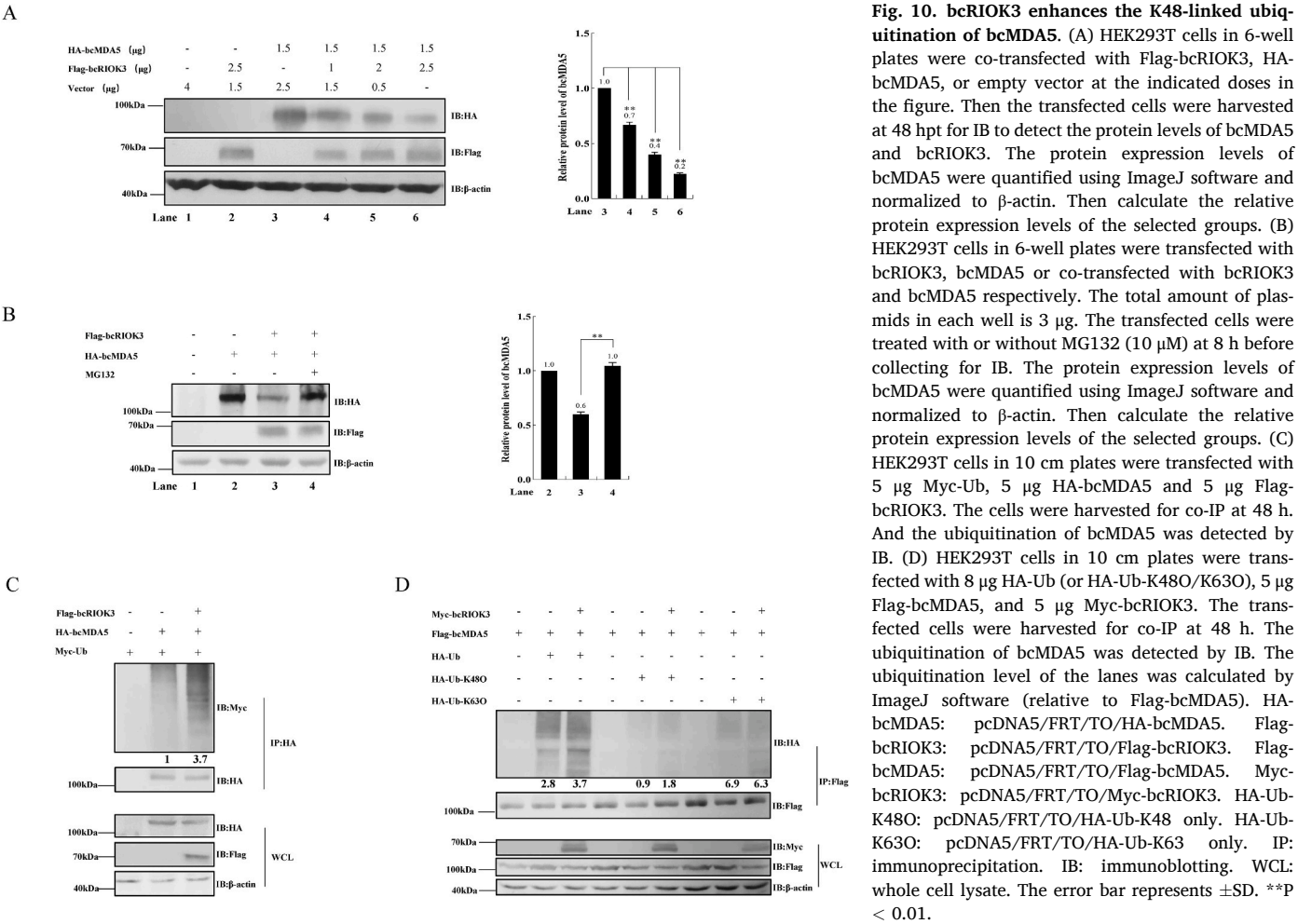

Fig. 10. bcRIOK3 enhances the K48-linked ubiquitination of bcMDA5. (A) HEK293T cells in 6-well plates were co-transfected with Flag-bcRIOK3, HA-bcMDA5, or empty vector at the indicated doses in the figure. Then the transfected cells were harvested at 48 hpt for IB to detect the protein levels of bcMDA5 and bcRIOK3. The protein expression levels of bcMDA5 were quantified using ImageJ software and normalized to β-actin. Then calculate the relative protein expression levels of the selected groups. (B) HEK293T cells in 6-well plates were transfected with bcRIOK3, bcMDA5 or co-transfected with bcRIOK3 and bcMDA5 respectively. The total amount of plasmids in each well is 3 μg. The transfected cells were treated with or without MG132 (10 μM) at 8 h before collecting for IB. The protein expression levels of bcMDA5 were quantified using ImageJ software and normalized to β-actin. Then calculate the relative protein expression levels of the selected groups. (C) HEK293T cells in 10 cm plates were transfected with 5 μg Myc-Ub, 5 μg HA-bcMDA5 and 5 μg Flag-bcRIOK3. The cells were harvested for co-IP at 48 h. And the ubiquitination of bcMDA5 was detected by IB. (D) HEK293T cells in 10 cm plates were transfected with 8 μg HA-Ub (or HA-Ub-K48O/K63O), 5 μg Flag-bcMDA5, and 5 μg Myc-bcRIOK3. The transfected cells were harvested for co-IP at 48 h. The ubiquitination of bcMDA5 was detected by IB. The ubiquitination level of the lanes was calculated by ImageJ software (relative to Flag-bcMDA5). HA-bcMDA5: pcDNA5/FRT/TO/HA-bcMDA5. Flag-bcRIOK3: pcDNA5/FRT/TO/Flag-bcRIOK3. Flag-bcMDA5: pcDNA5/FRT/TO/Flag-bcMDA5. Myc-bcRIOK3: pcDNA5/FRT/TO/Myc-bcRIOK3. HA-Ub-K48O: pcDNA5/FRT/TO/HA-Ub-K48 only. HA-Ub-K63O: pcDNA5/FRT/TO/HA-Ub-K63 only. IP: immunoprecipitation. IB: immunoblotting. WCL: whole cell lysate. The error bar represents ±SD. **P < 0.01.

Spring viremia of carp virus (SVCV) is the causative agent of SVC and causes significant mortality in *Cyprinidae* fish. The genome of SVCV encodes five proteins containing the nucleoprotein (N), phosphoprotein (P), matrix protein (M), glycoprotein (G), and viral RNA–dependent RNA polymerase (L) (Lu et al., 2016). It has been reported that SVCV-P protein is phosphorylated by a kinase, which decreases the phosphorylation of interferon regulator factor 3 (IRF3) and inhibits interferon production (Li et al., 2016). Another study revealed that SETD3 directly interacted with SVCV-P protein, initiating ubiquitination of SVCV-P and subsequent degradation of the SVCV-P protein (Zhao et al., 2023). Additionally, studies have demonstrated that SVCV-N protein targets MAVS for K48-linked ubiquitination, which promoted the degradation of MAVS(Lu et al., 2016). Recent research has shown that SVCV-M protein plays an inhibitory role in host IFN production by competitively recruiting TRAF3 from the MAVS signaling complex via inhibition of K63-linked polyubiquitination (Wang et al., 2022). These studies collectively indicate that SVCV-encoding proteins can interact with host proteins and regulate host immune responses through different mechanisms. Given these observations, we think it is worthwhile to further explore the potential interaction between bcRIOK3 and SVCV-encoding proteins, as well as to explore whether SVCV exploits bcRIOK3 for immune evasion in our future studies.

Taken together, our research revealed that bcRIOK3 negatively regulates the IFN signaling pathway by facilitating the degradation of bcMDA5 through the ubiquitin-proteasome degradation pathway. Our findings provide fresh perspectives on the regulation of IFN signaling in teleost.

Data availability

Data will be made available on request.

Acknowledgements

This work was supported by the National Natural Science Foundation of China (U21A20268, U22A20535, 31920103016, 32002415, 32002383), Hunan Provincial Science and Technology Department (2022JJ40276, 2023JJ40435), the Modern Agricultural Industry Program of Hunan Province, the Research and Development Platform of Fish Disease and Vaccine for Postgraduates in Hunan Province.

Appendix A. Supplementary data

Supplementary data to this article can be found online at https://doi.org/10.1016/j.dci.2023.105059.

References

Abe, Y., Fujii, K., Nagata, N., Takeuchi, O., Akira, S., Oshiumi, H., Matsumoto, M., Seya, T., Koike, S., 2012. The toll-like receptor 3-mediated antiviral response is important for protection against poliovirus infection in poliovirus receptor transgenic mice. J. Virol. 86 (1), 185–194. http://10.1128/jvi.05245-11.

Akira, S., Uematsu, S., Takeuchi, O., 2006. Pathogen recognition and innate immunity. Cell 124 (4), 783–801. http://10.1016/j.cell.2006.02.015.

Andrejeva, J., Childs, K.S., Young, D.F., Carlos, T.S., Stock, N., Goodbourn, S., Randall, R. E., 2004. The V proteins of paramyxoviruses bind the IFN-inducible RNA helicase, mda-5, and inhibit its activation of the IFN-beta promoter. Proc. Natl. Acad. Sci. U. S. A. 101 (49), 17264–17269. http://10.1073/pnas.0407639101.

Baumas, K., Soudet, J., Caizergues-Ferrer, M., Faubladier, M., Henry, Y., Mougin, A., 2012. Human RioK3 is a novel component of cytoplasmic pre-40S pre-ribosomal particles. RNA Biol. 9 (2), 162–174. http://10.4161/rna.18810.

Boehm, T., Iwanami, N., Hess, I., 2012. Evolution of the immune system in the lower vertebrates. Annu. Rev. Genom. Hum. Genet. 13, 127–149. http://10.1146/annurev-genom-090711-163747.

Brubaker, S.W., Bonham, K.S., Zanoni, I., Kagan, J.C., 2015. Innate immune pattern recognition: a cell biological perspective. Annu. Rev. Immunol. 33, 257–290. http://10.1146/annurev-immunol-032414-112240.

Bruns, A.M., Horvath, C.M., 2015. LGP2 synergy with MDA5 in RLR-mediated RNA recognition and antiviral signaling. Cytokine 74 (2), 198–206. http://10.1016/j.cyto.2015.02.010.

Cai, C., Liu, J., Tan, Y., Wei, J., Yang, X., Xiao, J., Feng, H., 2020. Black carp NAP1 positively regulates MDA5-mediated antiviral signaling during the innate immune activation. Dev. Comp. Immunol. 107, 103659. http://10.1016/j.dci.2020.103659.

Feng, J., De Jesus, P.D., Su, V., Han, S., Gong, D., Wu, N.C., Tian, Y., Li, X., Wu, T.T., Chanda, S.K., Sun, R., 2014. RIOK3 is an adaptor protein required for IRF3-mediated antiviral type I interferon production. J. Virol. 88 (14), 7987–7997. http://10.1128/jvi.00643-14.

Halfmann, R., Lindquist, S., 2008. Screening for amyloid aggregation by semi-denaturing detergent-agarose gel electrophoresis. J. Vis. Exp. 17. http://10.3791/838.

Honda, K., Yanai, H., Negishi, H., Asagiri, M., Sato, M., Mizutani, T., Shimada, N., Ohba, Y., Takaoka, A., Yoshida, N., Taniguchi, T., 2005. IRF-7 is the master regulator of type-I interferon-dependent immune responses. Nature 434 (7034), 772–777. http://10.1038/nature03464.

Hou, F., Sun, L., Zheng, H., Skaug, B., Jiang, Q.X., Chen, Z.J., 2011. MAVS forms functional prion-like aggregates to activate and propagate antiviral innate immune response. Cell 146 (3), 448–461. http://10.1016/j.cell.2011.06.041.

Huang, Y., Yang, M., Yu, Y., Yang, Y., Zhou, L., Huang, X., Qin, Q., 2016. Grouper TRIM13 exerts negative regulation of antiviral immune response against nodavirus. Fish Shellfish Immunol. 55, 106–115. http://10.1016/j.fsi.2016.05.029.

Kang, D.C., Gopalkrishnan, R.V., Wu, Q., Jankowsky, E., Pyle, A.M., Fisher, P.B., 2002. mda-5: an interferon-inducible putative RNA helicase with double-stranded RNA-dependent ATPase activity and melanoma growth-suppressive properties. Proc. Natl. Acad. Sci. U. S. A. 99 (2), 637–642. http://10.1073/pnas.022637199.

Kato, H., Takeuchi, O., Mikamo-Satoh, E., Hirai, R., Kawai, T., Matsushita, K., Hiiragi, A., Dermody, T.S., Fujita, T., Akira, S., 2008. Length-dependent recognition of double-stranded ribonucleic acids by retinoic acid-inducible gene-I and melanoma differentiation-associated gene 5. J. Exp. Med. 205 (7), 1601–1610. http://10.1084/jem.20080091.

Kimmelman, A.C., Hezel, A.F., Aguirre, A.J., Zheng, H., Paik, J.H., Ying, H., Chu, G.C., Zhang, J.X., Sahin, E., Yeo, G., Ponugoti, A., Nabioullin, R., Deroo, S., Yang, S., Wang, X., McGrath, J.P., Protopopova, M., Ivanova, E., Zhang, J., Feng, B., Tsao, M. S., Redston, M., Protopopov, A., Xiao, Y., Futreal, P.A., Hahn, W.C., Klimstra, D.S., Chin, L., DePinho, R.A., 2008. Genomic alterations link Rho family of GTPases to the highly invasive phenotype of pancreas cancer. Proc. Natl. Acad. Sci. U. S. A. 105 (49), 19372–19377. http://10.1073/pnas.0809966105.

Li, J., Sun, R., He, L., Sui, G., Di, W., Yu, J., Su, W., Pan, Z., Zhang, Y., Zhang, J., Ren, F., 2022. A systematic pan-cancer analysis identifies RIOK3 as an immunological and prognostic biomarker. Am J Transl Res 14 (6), 3750–3768.

Li, S., Lu, L.F., Wang, Z.X., Lu, X.B., Chen, D.D., Nie, P., Zhang, Y.A., 2016. The P protein of spring viremia of carp virus negatively regulates the fish interferon response by inhibiting the kinase activity of TANK-binding kinase 1. J. Virol. 90 (23), 10728–10737. http://10.1128/JVI.01381-16.

Liao, G., Liu, J., Yin, L., He, Y., Qiao, G., Song, W., He, Y., Deng, Z., Xiao, J., Feng, H., 2022. DAK inhibits MDA5-mediated signaling in the antiviral innate immunity of black carp. Dev. Comp. Immunol. 126, 104255. http://10.1016/j.dci.2021.104255.

Liu, J., Li, J., Xiao, J., Chen, H., Lu, L., Wang, X., Tian, Y., Feng, H., 2017. The antiviral signaling mediated by black carp MDA5 is positively regulated by LGP2. Fish Shellfish Immunol. 66, 360–371. http://10.1016/j.fsi.2017.05.035.

Loo, Y.M., Gale Jr., M., 2011. Immune signaling by RIG-I-like receptors. Immunity 34 (5), 680–692. http://10.1016/j.immuni.2011.05.003.

Lu, L.F., Li, S., Lu, X.B., LaPatra, S.E., Zhang, N., Zhang, X.J., Chen, D.D., Nie, P., Zhang, Y.A., 2016. Spring viremia of carp virus N protein suppresses fish IFNφ1 production by targeting the mitochondrial antiviral signaling protein. J. Immunol. 196 (9), 3744–3753. http://10.4049/jimmunol.1502038.

Mishra, D.K., Chen, Z., Wu, Y., Sarkissyan, M., Koeffler, H.P., Vadgama, J.V., 2010. Global methylation pattern of genes in androgen-sensitive and androgen-independent prostate cancer cells. Mol. Cancer Therapeut. 9 (1), 33–45. http://10.1158/1535-7163.Mct-09-0486.

Patel, J.R., García-Sastre, A., 2014. Three-stranded antiviral attack. Elife 3, e02369. http://10.7554/eLife.02369.

Paudel, R.R., Lu, D., Roy Chowdhury, S., Monroy, E.Y., Wang, J., 2023. Targeted protein degradation via lysosomes. Biochemistry 62 (3), 564–579. http://10.1021/acs.biochem.2c00310.

Rehwinkel, J., Reis e Sousa, C., 2010. RIGorous detection: exposing virus through RNA sensing. Science 327 (5963), 284–286. http://10.1126/science.1185068.

Rothenfusser, S., Goutagny, N., DiPerna, G., Gong, M., Monks, B.G., Schoenemeyer, A., Yamamoto, M., Akira, S., Fitzgerald, K.A., 2005. The RNA helicase Lgp2 inhibits TLR-independent sensing of viral replication by retinoic acid-inducible gene-I. J. Immunol. 175 (8), 5260–5268. http://10.4049/jimmunol.175.8.5260.

Seth, R.B., Sun, L., Ea, C.K., Chen, Z.J., 2005. Identification and characterization of MAVS, a mitochondrial antiviral signaling protein that activates NF-kappaB and IRF 3. Cell 122 (5), 669–682. http://10.1016/j.cell.2005.08.012.

Singleton, D.C., Rouhi, P., Zois, C.E., Haider, S., Li, J.L., Kessler, B.M., Cao, Y., Harris, A. L., 2015. Hypoxic regulation of RIOK3 is a major mechanism for cancer cell invasion and metastasis. Oncogene 34 (36), 4713–4722. http://10.1038/onc.2014.396.

Takaki, H., Watanabe, Y., Shingai, M., Oshiumi, H., Matsumoto, M., Seya, T., 2011. Strain-to-strain difference of V protein of measles virus affects MDA5-mediated IFN-β-inducing potential. Mol. Immunol. 48 (4), 497–504. http://10.1016/j.molimm.2010.10.006.

Takashima, K., Oshiumi, H., Takaki, H., Matsumoto, M., Seya, T., 2015. RIOK3-mediated phosphorylation of MDA5 interferes with its assembly and attenuates the innate immune response. Cell Rep. 11 (2), 192–200. http://10.1016/j.celrep.2015.03.027.

Thaiss, C.A., Levy, M., Itav, S., Elinav, E., 2016. Integration of innate immune signaling. Trends Immunol. 37 (2), 84–101. http://10.1016/j.it.2015.12.003.

Wang, C., Li, J., Yang, X., Wang, Q., Zhong, H., Liu, Y., Yan, W., He, Y., Deng, Z., Xiao, J., Feng, H., 2021. Black carp IKKε collaborates with IRF3 in the antiviral signaling. Fish Shellfish Immunol. 118, 160–168. http://10.1016/j.fsi.2021.08.034.

Wang, C., Peng, J., Zhou, M., Liao, G., Yang, X., Wu, H., Xiao, J., Feng, H., 2019a. TAK1 of black carp positively regulates IRF7-mediated antiviral signaling in innate immune activation. Fish Shellfish Immunol. 84, 83–90. http://10.1016/j.fsi.2018.09.075.

Wang, J., Varin, T., Vieth, M., Elkins, J.M., 2019b. Crystal structure of human RIOK2 bound to a specific inhibitor. Open Biol 9 (4), 190037. http://10.1098/rsob.190037.

Wang, Y.Y., Chen, Y.L., Ji, J.F., Fan, D.D., Lin, A.F., Xiang, L.X., Shao, J.Z., 2022. Negative regulatory role of the spring viremia of carp virus matrix protein in the host interferon response by targeting the MAVS/TRAF3 signaling Axis. J. Virol. 96 (16), e0079122. http://10.1128/jvi.00791-22.

Wu, X.M., Zhang, J., Li, P.W., Hu, Y.W., Cao, L., Ouyang, S., Bi, Y.H., Nie, P., Chang, M. X., 2020. NOD1 promotes antiviral signaling by binding viral RNA and regulating the interaction of MDA5 and MAVS. J. Immunol. 204 (8), 2216–2231. http://10.4049/jimmunol.1900667.

Xu, H., He, X., Zheng, H., Huang, L.J., Hou, F., Yu, Z., de la Cruz, M.J., Borkowski, B., Zhang, X., Chen, Z.J., Jiang, Q.X., 2014. Structural basis for the prion-like MAVS filaments in antiviral innate immunity. Elife 3, e01489. http://10.7554/eLife.01489.

Yang, C., Liu, L., Liu, J., Ye, Z., Wu, H., Feng, P., Feng, H., 2019. Black carp IRF5 interacts with TBK1 to trigger cell death following viral infection. Dev. Comp. Immunol. 100, 103426. http://10.1016/j.dci.2019.103426.

Yoneyama, M., Kikuchi, M., Matsumoto, K., Imaizumi, T., Miyagishi, M., Taira, K., Foy, E., Loo, Y.M., Gale Jr., M., Akira, S., Yonehara, S., Kato, A., Fujita, T., 2005. Shared and unique functions of the DExD/H-box helicases RIG-I, MDA5, and LGP2 in antiviral innate immunity. J. Immunol. 175 (5), 2851–2858. http://10.4049/jimmunol.175.5.2851.

Yoneyama, M., Kikuchi, M., Natsukawa, T., Shinobu, N., Imaizumi, T., Miyagishi, M., Taira, K., Akira, S., Fujita, T., 2004. The RNA helicase RIG-I has an essential function in double-stranded RNA-induced innate antiviral responses. Nat. Immunol. 5 (7), 730–737. http://10.1038/ni1087.

Zhao, X., Ji, N., Guo, J., Huang, W., Feng, J., Shi, Y., Chen, K., Wang, J., Zou, J., 2023. Zebrafish SETD3 mediated ubiquitination of phosphoprotein limits spring viremia of carp virus infection. Fish Shellfish Immunol. 139, 108870. http://10.1016/j.fsi.2023.108870.

Zhou, W., Zhou, J., Lv, Y., Qu, Y., Chi, M., Li, J., Feng, H., 2015. Identification and characterization of MAVS from black carp Mylopharyngodon piceus. Fish Shellfish Immunol. 43 (2), 460–468. http://10.1016/j.fsi.2015.01.016.